

The DNA-binding Domain of Human Papillomavirus Type 18 E1

CRYSTAL STRUCTURE, DIMERIZATION, AND DNA BINDING*

Received for publication, October 24, 2003

Published, JBC Papers in Press, October 30, 2003, DOI 10.1074/jbc.M311681200

Anitra S. Auster^{‡§} and Leemor Joshua-Tor^{‡¶}

From the [‡]W. M. Keck Structural Biology Laboratory, Cold Spring Harbor Laboratory, Cold Spring Harbor, New York 11724 and the [§]Graduate Program in Genetics, Stony Brook University, Stony Brook, New York 11794

High risk types of human papillomavirus, such as type 18 (HPV-18), cause cervical carcinoma, one of the most frequent causes of cancer death in women worldwide. DNA replication is one of the central processes in viral maintenance, and the machinery involved is an excellent target for the design of antiviral therapy. The papillomaviral DNA replication initiation protein E1 has origin recognition and ATP-dependent DNA melting and helicase activities, and it consists of a DNA-binding domain and an ATPase/helicase domain. While monomeric in solution, E1 binds DNA as a dimer. Dimerization occurs via an interaction of hydrophobic residues on a single α -helix of each monomer. Here we present the crystal structure of the monomeric HPV-18 E1 DNA-binding domain refined to 1.8-Å resolution. The structure reveals that the dimerization helix is significantly different from that of bovine papillomavirus type 1 (BPV-1). However, we demonstrate that the analogous residues required for E1 dimerization in BPV-1 and the low risk HPV-11 are also required for HPV-18 E1. We also present evidence that the HPV-18 E1 DNA-binding domain does not share the same nucleotide and amino acid requirements for specific DNA recognition as BPV-1 and HPV-11 E1.

and most frequent cancer in women worldwide and a major cause of death in countries that lack screening programs (1). HPV-16 accounts for 50–60% of all cervical cancer cases and is the predominant type in carcinomas of squamous cell origin (2). HPV-18 accounts for 10–12% of all cervical cancers and is the predominant type in adenocarcinomas and small cell neuroendocrine carcinomas of the cervix (2, 3). Adenocarcinomas are difficult to detect by the Papanicolaou (Pap) smear, and therefore cancer commonly associated with HPV-18 is often associated with rapidly progressing disease and death (3). High risk HPVs also play a role in cancers of the prostate, bladder, anus, penis, larynx, esophagus, oral cavity, and skin. Current treatment options for HPV lesions do not specifically target HPV infection, resulting in treatment failures and disease recurrence and/or progression.

All types of papillomavirus are tropic for epithelial cells of skin and mucous membranes. The 8-kilobase pair genome encodes for six early (E) genes, involved in viral DNA replication, viral gene transcription, and cellular transformation, and two late (L) genes, which form the viral capsid. Stages in the viral life cycle are dependent on specific factors that are present in sequential differentiated stages of epithelial cells with expression of L genes restricted to the outermost layer of differentiated keratinocytes. While cervical cancer cells contain chromosomally integrated HPV DNA or a mixture of both integrated and episomal DNA, in non-cancerous or premalignant warts, the HPV genome is strictly episomal (4). HPV episomes associate with cellular histones in a chromatin-like assembly. The primary viral proteins expressed in the basal cells are E1 and E2, which are both essential for initiation of papillomavirus DNA replication *in vivo* (5, 6). DNA replication is one of the central processes in viral maintenance, and the machinery involved would be a good target for the design of antiviral therapy at benign and premalignant stages of disease.

E1 is involved in all steps of replication initiation: origin (*ori*) recognition, ATP-dependent DNA melting, and unwinding of DNA (for a review, see Ref. 7). The protein is highly conserved among papillomaviruses and consists of a DNA-binding domain (DBD) and an ATPase/helicase domain. We previously determined the crystal structure of the BPV-1 E1-DBD (residues 159–303) (8) and found it to be structurally similar to the DBD of SV40 large T antigen, although sequence conservation is only 6%. Others have reported structural similarities with additional viral proteins essential for DNA replication and integration, such as the DBD of the geminivirus tomato yellow leaf curl virus Rep and the endonuclease domain of adeno-associated virus Rep (9, 10).

While monomeric in solution, full-length E1 must first bind to the viral *ori* as a dimer along with a dimer of E2 (11). The DBD of E1 alone is highly sequence-specific, but in the context of full-length protein, which also contains the nonspecific DNA

Papillomavirus is classified in the Papovaviridae family of double-stranded DNA tumor viruses, which also includes polyomaviruses such as SV40. There are about 100 identified papillomaviruses that infect humans. The clinical lesions range from benign warts to invasive cancers depending on the type of human papillomavirus (HPV)¹ and several host factors. Recently HPV-16, -18, and other high risk HPVs have been implicated as the necessary cause of cervical carcinoma, the sec-

* This work was supported by National Institutes of Health Grant AI46724 and by the Louis Morin Charitable Trust (to L. J.). Research carried out at the National Synchrotron Light Source at Brookhaven National Laboratory was supported by the United States Department of Energy, Division of Materials Sciences and Division of Chemical Sciences, under Contract No. DE-AC02-98CH10886. The costs of publication of this article were defrayed in part by the payment of page charges. This article must therefore be hereby marked "advertisement" in accordance with 18 U.S.C. Section 1734 solely to indicate this fact.

The atomic coordinates and structure factors (code 1R9W) have been deposited in the Protein Data Bank, Research Collaboratory for Structural Bioinformatics, Rutgers University, New Brunswick, NJ (<http://www.rcsb.org/>).

¶ To whom correspondence should be addressed: Cold Spring Harbor Laboratory, 1 Bungtown Rd., Cold Spring Harbor, NY 11724. Tel.: 516-367-8821; Fax: 516-367-8873; E-mail: leemor@cshl.edu.

¹ The abbreviations used are: HPV, human papillomavirus; HPV-16, HPV type 16; HPV-18, HPV type 18; HPV-11, HPV type 11; E, early; L, late; *ori*, origin of replication; DBD, DNA-binding domain; BPV-1, bovine papillomavirus type 1; BS, binding site; GST, glutathione S-transferase; HA, hemagglutinin; r.m.s.d., root mean square deviation.

binding activity of the E1 helicase domain, E1 requires interactions with E2 to block nonspecific E1/DNA interactions (12). Recently inhibitors of the E1/E2 interaction have been reported to inhibit *in vivo* DNA replication for low risk HPV types 6 and 11 but not for high risk HPVs (13).

Once the initial E1 dimer has been loaded by E2, more molecules of E1 are recruited by E2 bound at a distal site to form a tetrameric E1 complex (14). Ultimately two hexameric E1 helicases are assembled that have ATPase activity and can unwind the DNA (5, 14). We have also previously determined the crystal structures of the BPV-1 E1-DBD dimer bound to DNA and tetramer bound to DNA (15), and the ringlike hexameric helicase form of E1 has been visualized by electron microscopy (16).

E1 dimerization is due to the interaction of hydrophobic residues in the third α -helix of each monomer. The interface is small, burying only 500 Å² of monomer surface area (8). While the hydrophobicity of the dimer interface is conserved among all papillomavirus types, the actual residues involved are very poorly conserved. However, this interaction is crucial to replication initiation as mutation of one hydrophobic residue in BPV-1 E1-DBD (Val-202 or Ala-206) or HPV-11 E1-DBD (Ala-251) to arginine inhibits the ability of E1-DBD to bind to *ori* DNA as a dimer *in vitro*, and in the context of full-length E1, these mutations prevent DNA replication *in vivo* (8, 17).² The E1 dimerization interface is a logical target for the disruption of DNA replication by a small molecule because of its limited surface area and functional importance. In this study, we present the structure of the E1-DBD from the high risk HPV-18 and provide evidence that E1 dimerization via the α 3 helix is conserved, although the conformation of the α 3 helix differs from that of BPV-1 E1. This structural information is important for the development of specific antiviral therapeutics to this clinically relevant group of viruses.

E1 binds to overlapping sites in the *ori* in the assembly of E1 complexes (18, 19). The initial E1-DBD dimer binds cooperatively, as shown for BPV-1 and HPV-11, to palindromic hexanucleotide sites (called sites 2 and 4, see Table I) that are separated by 3 base pairs in the *ori* and have the consensus sequence ATTGTT (17, 19). These sites encompass two consecutive major grooves of DNA, one helical turn apart, and binding of the E1-DBD dimer results in compression of the minor groove and increased positive rise, twist, and slide and negative roll of the DNA in the BPV-1 E1-DBD/DNA co-crystal structure (15). Circular permutation assays have indicated that binding of the BPV-1 E1-DBD dimer confers a bend of 40–50° in the DNA (20), and hydroxy radical footprinting experiments have demonstrated that DNA sequences extending beyond the E1 binding sites (BSs) are involved in E1 binding and DNA bending (21).

The DNA-binding region of E1 consists of the fourth α -helix and a well ordered loop, which form a continuous area on the surface of the protein but bind separately to the two individual strands of the DNA (15). The DNA-binding helix makes only nonspecific phosphate backbone interactions, while the DNA-binding loop is responsible for all base-specific contacts (15). The residues that contact the DNA are very well conserved between all papillomaviruses. All of the base-specific contacts are van der Waals interactions, and they primarily involve the thymidine in position 2 of each hexanucleotide site. One specific protein-DNA contact (shown for BPV-1) is a threonine in the DNA-binding loop (Thr-187) with the methyl group of this thymidine (15, 22). DNA binding is abrogated if Thr-187 is changed to an alanine or if the thymidine in position 2 of either

TABLE I
E1 binding sites from 20 papillomaviruses

	SITE 4	SITE 2		SITE 4	SITE 2
BPV-1	ATTGTTGTT TAACAACAA	AACAATAAT TTGTATTA	HPV-32	GTATTATATA CAATAATAT	AAGTATAAT TTCATATA
HPV-1	ATGGTAGTT TACCATCAA	AACAACAAC TTGTGTG	HPV-33	ATTATAGTT TAATATCAA	TACTATTAT ATGATAATA
HPV-4	ATGATAGTT TACTATCAA	GGCAACAAT CCGTGTTA	HPV-34	ATTATAAAA TAATATTTT	AACATAAAT TTGATATA
HPV-6	ATTGTTAAT TAACAATAA	AACATAAAC TTGATATTC	HPV-35	ATTATAGTT TAATATCAA	AGTAACAAT TCATGTTA
HPV-7	GTTATTATG CAATAATAC	TTTAATAAT AAATATTA	HPV-40	CTTATTATT GAATAATAA	AATAACAAT TTATGTTA
HPV-11	ATTGTTTAT TAACAATAA	AACATAAAG TTGATATTC	HPV-51	CTTATAACA GAATATTGT	TTTAACAAT AAATGTTA
HPV-13	ATTGTTAGA TAACAATCT	AACATAAT TTGATAATA	HPV-52	ATTATAAAT TAATATTA	TATAAATAT ATATAATA
HPV-16	ATTGTAGTT TAACATCAA	TAGTATTAT ATCATATA	HPV-58	ATTATAGTT TAATATCAA	TAGTATTAT ATCATATA
HPV-18	ATTGTTAAA TAACAATTT	AGTATTAAT TCATAATTA	HPV-63	GTTGTTGTT CAACAACAA	AACAACAT TTGTGATA
HPV-31	ATTATTATT TAATAATAA	AAGTATAAA TTCATATT	HPV-65	ATGATAGTT TACTATCAA	GGCAACAAC CCGTGTG

E1-BS, site 2 or 4, is changed to any other base, including a change to uridine, which removes only the methyl group. This is the only nucleotide position that has an absolute requirement for a particular base (shown for BPV-1 and HPV-11) (15, 17), and this thymidine (shown in red in Table I) is in fact conserved among many papillomavirus sequences. However, the hexanucleotide sequence of site 2 in the HPV-18 *ori* deviates and instead has a T-to-A transversion in position 2 (shown in blue in Table I). In this study, we present evidence that the thymidine in BS2 is dispensable for HPV-18 E1 DNA recognition although the thymidine in BS4 is significant, and the threonine in the DNA-binding loop equivalent to BPV-1 Thr-187 (HPV-18 Thr-238) is also nonessential for HPV-18 E1 DNA binding. The differences in DNA binding may be related to the structural differences at the HPV-18 E1 dimerization interface and/or differences in the electrostatic potential energy surface of the HPV-18 E1-DBD.

EXPERIMENTAL PROCEDURES

Protein Expression, Site-directed Mutagenesis, and Purification—The plasmid for expression of the minimal HPV-18 E1-DBD (amino acids 210–354) as a glutathione *S*-transferase (GST) fusion protein with an internal thrombin cleavage site was provided by Arne Stenlund (Cold Spring Harbor Laboratory). The plasmid encoding an additional HPV-18 E1 fragment (amino acids 193–425) was cloned from genomic DNA (ATCC) into the BamHI and XhoI sites of pGEX-4T-1 (Amersham Biosciences), resulting in an N-terminal GST-tagged protein with an internal thrombin cleavage site. Plasmids for expression of the HPV-18 E1-(193–425) fragment with N-terminal hemagglutinin (HA) or FLAG tags were cloned by insertion of a cassette containing the respective epitope tag between the thrombin cleavage site and the first codon of the protein. Single amino acid substitutions were introduced in vectors encoding untagged, HA-tagged, and FLAG-tagged HPV-18 E1-(193–425) using the QuikChange site-directed mutagenesis kit (Stratagene) according to the manufacturer's instructions.

All HPV-18 E1-DBD fragments were expressed in *Escherichia coli* strain BL21DE3 at 17 °C by induction with 0.4 mM isopropyl-1-thio- β -D-galactopyranoside for 12 h. The proteins were purified using the procedure described previously for the BPV-1 E1-DBD (8).

Crystallization, Data Collection, Structure Solution, and Refinement—Crystals were grown by the hanging drop method at 17 °C using a 5 mg/ml protein solution containing 20 mM HEPES, pH 7.5, 100 mM NaCl, and 10 mM dithiothreitol and a reservoir solution consisting of

² A. Stenlund, personal communication.

TABLE II
Data collection and refinement statistics

Wavelength (Å)	1.1
Oscillation angle (°)	1.0
Space group	C2
Cell dimensions	$a = 70.54 \text{ \AA}$, $b = 46.24 \text{ \AA}$, $c = 43.19 \text{ \AA}$
	$\beta = 94.01^\circ$
Resolution (Å) ^a	30.0–1.8 (1.91–1.8)
Observed reflections	45,127
Unique reflections	12,094 (1412)
Redundancy	3.41 (2.25)
Completeness ^a	93.0 (69.1)
$\langle I/\sigma(I) \rangle^a$	17.5 (5.7)
$R_{\text{merge}}^{a,b}$	0.049 (0.135)
R factor (%)	21.3
R_{free} (%)	22.2
Number of atoms (protein, solvent)	1202, 109
r.m.s.d. from bond ideality (Å)	0.009
r.m.s.d. from angle ideality (°)	1.5
Protein average B factor (Å ²)	19.4
Ramachandran plot	
Most favorable (%)	98.3
Additionally allowed (%)	1.7

^a Numbers in parentheses are for the highest resolution shell.

^b $R_{\text{merge}} = \sum I - \langle I \rangle / \sum I$ where I = observed intensity and $\langle I \rangle$ = average intensity obtained from symmetry-related and multiple measurements.

28–30% polyethylene glycol 4000, 100 mM ammonium acetate, 100 mM sodium citrate, pH 5.0–5.6, and 50–100 mM dithiothreitol in a 1:1 (protein:reservoir) ratio for a drop volume of 2 μ l. Crystals with typical dimensions around 0.1 \times 0.05 \times 0.05 mm grew within 2 weeks.

Data were collected at beamline X26C at the National Synchrotron Light Source at Brookhaven National Laboratory at 100 K by flash-freezing crystals directly in the cryostream. See Table II for data collection statistics. Diffraction data were processed and scaled with HKL2000 (23).

The structure was solved by molecular replacement with the program MOLREP (24) (resolution range 30–3 Å) using a search model based on the crystal structure of the minimal E1-DBD from BPV-1 (amino acids 159–303) (8) in which non-identical residues were changed to alanine. The initial R factor was 0.527, and the correlation coefficient was 0.267. The B factors of the starting model were set to 19 Å² according to the Wilson plot. The model phases were used as the starting phases for the solvent-flattening routine of CNS (25). The model was then refined against the data with CNS followed by iterative model building using O (26). 5% of reflections were randomly reserved for calculating the R_{free} at all stages to monitor refinement. Several cycles of model building and refinement allowed for the placement of water molecules and two alternate side chain conformations to produce the final model. The criteria for the assignment of a $F_o - F_c$ density peak as water is a peak height greater than 4 σ and a hydrogen bonding distance between the solvent peak and any protein oxygen or nitrogen atom between 2.5 and 3.5 Å. The water scrutinizer routine of XPAND was used to check the validity of water molecules (27). The final model contains clear electron density for residues 210–353 with a break in the density from residues 231 to 239. Three residues (Gly, Ser, and Arg) that remain on the N terminus after cleavage of the protein from GST are not clearly visible in the electron density. See Table II for refinement details. Figures were prepared with MOLSCRIPT (28), BOBSCRIPT (29), and Raster 3D (30, 31).

Gel Mobility Shift Assays—The 105-bp probe for gel mobility shift assays was generated by PCR amplification of HPV-18 genomic DNA containing the *ori* using a plus strand primer that was 5'-labeled with [γ -³²P]ATP and T4 polynucleotide kinase. The probe was gel-purified by 8% non-denaturing PAGE, exposure to film, and elution of DNA from acrylamide slices by overnight incubation in Tris-EDTA.

For DNA competition assays, 21-bp DNA containing wild type HPV-18, mutant HPV-18, or BPV-1 E1 binding sites as found in the respective origins of replication was synthesized by Operon with the trityl protecting group left on and purified by reverse-phase chromatography, on-column deprotection, desalting, and ion exchange chromatography.

Competition assays were performed as described previously (32). Serial dilutions of competitor DNA were incubated with 10 ng of HPV-18 E1-DBD (amino acids 193–425) for 15 min at room temperature in a buffer containing 20 mM potassium phosphate, pH 7.4, 200 mM sodium chloride to minimize nonspecific E1/DNA interactions, 1 mM EDTA, 10% glycerol, 0.1% Nonidet P-40, 3 mM dithiothreitol, and 0.7 mg/ml bovine serum albumin. The reaction buffer for gel shift assays

with dimerization mutant proteins (data not shown) contained 100 mM NaCl, and HA-tagged proteins were supershifted with monoclonal antibody anti-HA tag (12CA5, produced and purified by the Antibody Facility of Cold Spring Harbor Laboratory). After preincubation, the radiolabeled probe (25,000 cpm/reaction) and 40 ng/reaction nonspecific competitor DNA (pGEX-4T-1) were added to each reaction. Samples were incubated at room temperature for an additional 30 min and then were resolved by 5% PAGE 39:1 (acrylamide:bisacrylamide) in 0.5 \times Tris-Borate-EDTA. After electrophoresis, the gels were dried and subjected to autoradiography.

Immunoprecipitation and Western Blot Analysis—Immunoprecipitation of FLAG fusion proteins and associated proteins was performed with anti-FLAG M2 affinity gel according to the manufacturer's protocol (Sigma). Binding reactions and washes were carried out in 20 mM HEPES, pH 7.5, and sodium chloride at the concentrations indicated in Fig. 3. Proteins were eluted into Laemmli sample buffer and loaded onto 15% SDS-polyacrylamide gels followed by transfer to Hybond-P membranes (Amersham Biosciences) using a semi-dry transfer apparatus. Blocking and antibody incubations were all carried out in 5% (w/v) nonfat milk in Tris-buffered saline with 0.1% Tween 20, and washes were with Tris-buffered saline with 0.1% Tween 20. The primary antibody was anti-FLAG polyclonal (Sigma) at a concentration of 1:1000, and the secondary antibody was goat anti-rabbit IgG (heavy + light)-horseradish peroxidase conjugate (Bio-Rad) at a concentration of 1:3000. Proteins were detected by incubation with Super Signal West Pico chemiluminescent reagent (Pierce) followed by exposure to x-ray film.

RESULTS

Overall Structure of the HPV-18 E1-DBD and Comparison with BPV-1 E1-DBD—The minimal stable DBD in BPV-1 E1 (residues 159–303) was identified by limited proteolysis, determined by gel mobility shift analysis to have DNA binding activity, and shown to possess a fold unique to viral *ori*-binding proteins (8–10). Because the sequence identity between BPV-1 E1-DBD and the analogous E1-DBD from several high risk HPVs, including HPV-18, is limited to 30–35% (Fig. 1A) and because of the difference in the HPV-18 E1-BS as compared with other papillomaviral origins of replication (Table I), we wanted to study whether there are any structural and/or biochemical differences among these proteins.

We expressed the HPV-18 E1-DBD (residues 210–354) as a GST fusion protein, cleaved the E1-DBD from GST, and purified the protein to homogeneity. The crystal structure of HPV-18 E1-DBD (residues 210–354), containing one molecule in the asymmetric unit, was solved by molecular replacement and refined to 1.8-Å resolution. As expected, the structure has the same overall fold as the E1-DBD from BPV-1, namely a central five-stranded antiparallel β -sheet flanked by four loosely packed α -helices on one side and two tightly packed helices on the other side (Fig. 1B). While the DNA-binding loop was very well ordered in the BPV-1 E1-DBD monomer structure, it is disordered in the structure of the HPV-18 E1-DBD. The BPV-1 E1-DBD monomer crystals grew from a high salt condition, and the ions in the solution were bound to the DNA-binding loop, mimicking some of the phosphates of a DNA backbone, as later seen from the co-crystal structure with DNA (15). However, the HPV-18 E1-DBD crystals grew from a low salt condition, so this effect was not present.

The overall root mean square deviation (r.m.s.d.) between the DBD of HPV-18 E1 and BPV-1 E1 is 1.13 Å for 132 aligned α -carbons (LSQMAN (33)). As shown in Fig. 1C, there are four regions for which the two molecules do not superimpose as well: the disordered DNA-binding loop (HPV-18 E1-DBD residues 231–239), an extended β -hairpin of no known function (residues 272–283), a small loop of no known function (residues 334–337), and the α 3 helix shown to be required for BPV-1² (8) and HPV-11 (17) DNA-dependent E1 dimerization and replication function (residues 252–263). The HPV-18 E1-DBD α 3 helix is a residue shorter in length than the analogous BPV-1 E1-DBD α 3 helix (residues 201–213) (8). Also, as seen in Fig. 1B, the HPV-18 E1-DBD α 3 helix has an obvious kink, which is

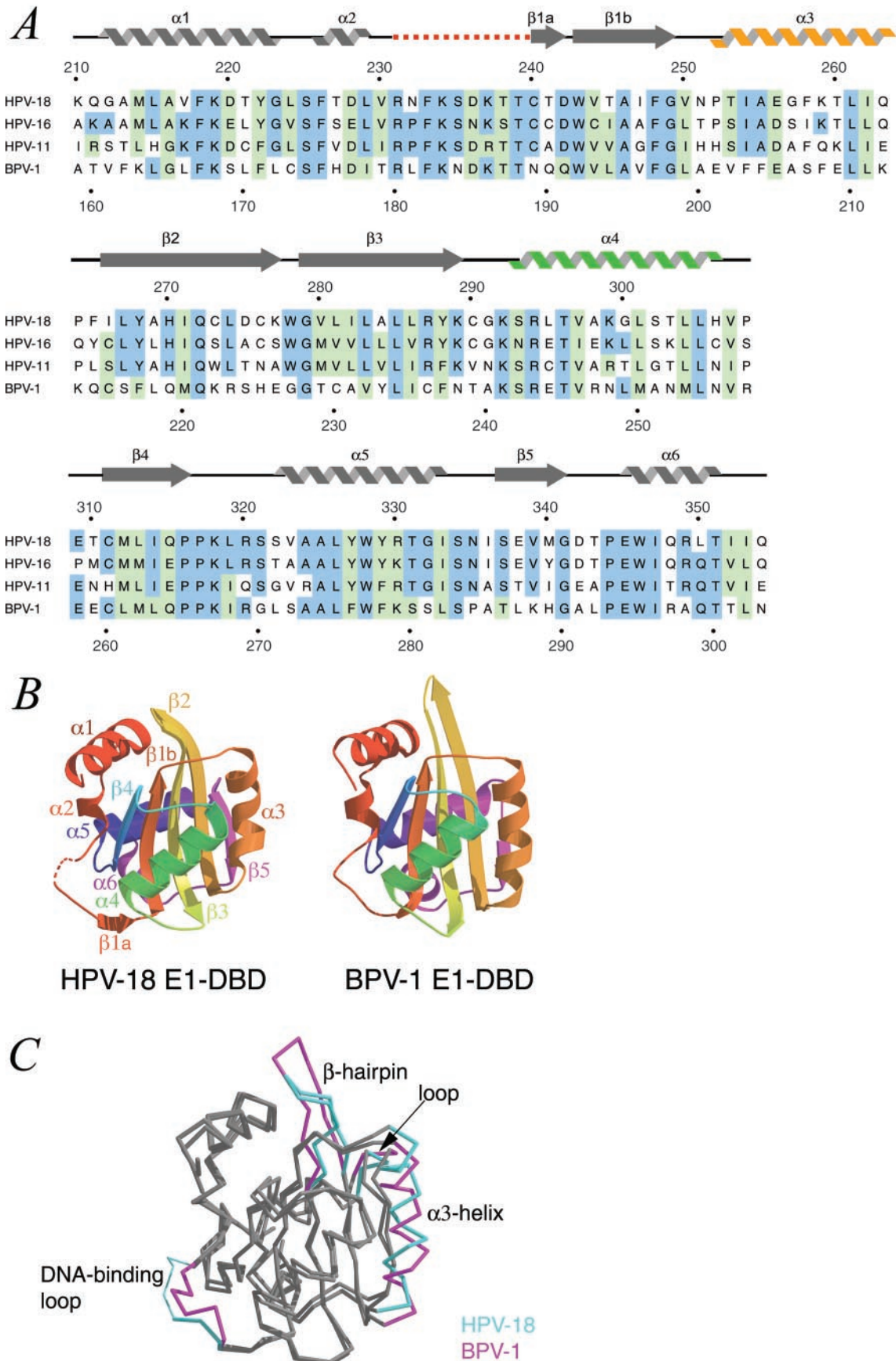


FIG. 1. Comparison of HPV-18 and BPV-1 E1-DBD sequences and structures. *A*, alignment of four selected papillomavirus E1-DBD sequences with the crystallographically determined secondary structure for HPV-18 E1-DBD on the top. As colored in *B*, the disordered DNA-binding loop is indicated by the red dashed line, the $\alpha 3$ dimerization helix is drawn in orange, and the $\alpha 4$ DNA-binding helix is drawn in green. Based on an alignment of a total of eight sequences (not shown: E1-DBD from HPV-31, -33, -12, and -5), residues that are identical among at least three sequences are highlighted in blue, and residues that are similar are highlighted in green. HPV-18 and BPV-1 E1-DBD residues are respectively numbered. *B*,

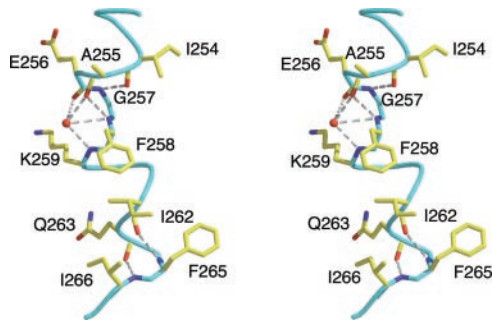


FIG. 2. **Hydrogen-bonding network of the HPV-18 E1-DBD $\alpha 3$ dimerization helix.** Stereodiagram of the $\alpha 3$ helix in HPV-18 E1-DBD. The kink in the HPV-18 E1-DBD $\alpha 3$ helix (in cyan) is due to backbone ($n + 3$) hydrogen bonds and hydrogen bonds to a water molecule (represented by the red ball). Hydrogen bonds are indicated by the dashed lines. The figure is rotated by 180° along the y axis with respect to the view in Fig. 1B for clarity.

clearly defined in the electron density, that is not present in the BPV-1 E1-DBD. The DNA-binding helix is unchanged between HPV-18 and BPV-1 E1-DBD.

The kink in the HPV-18 E1-DBD $\alpha 3$ helix is due to differences in the hydrogen (H)-bonding network (see Fig. 2). A straight α -helix retains its shape because of the backbone H-bonding interaction between the CO group of each residue n with the NH group of residue $(n + 4)$. In the HPV-18 E1-DBD $\alpha 3$ helix, there are four residues that H-bond with the NH group of the $(n + 3)$ residue rather than the $(n + 4)$: Ile-254 with Gly-257, Ala-255 with Phe-258, Ile-262 with Phe-265, and Gln-263 with Ile-266 (HBPLUS (34)), resulting in a partial 3_{10} helix. In contrast, the $\alpha 3$ helix in the BPV-1 E1-DBD structure consists of only $(n + 4)$ backbone H-bonding interactions of a typical, straight α -helix. The HPV-18 E1 $\alpha 3$ helix is also stabilized by a tightly bound water molecule, which H-bonds to the CO groups of residues Ala-255 and Glu-256 and the NH groups of residues Phe-258 and Lys-259 (XPAND (27)). However, in the BPV-1 E1-DBD structure there is no solvent bound to $\alpha 3$ helix residues. Finally residue Thr-253 in the HPV-18 E1-DBD $\alpha 3$ helix does not participate in any H-bonding interactions either to other residues or to solvent, whereas the equivalent residue (Val-202) in the BPV-1 E1-DBD makes the typical $(n + 4)$ H-bonds.

For BPV-1, there were four different interaction surfaces between E1-DBD monomers in the E1-DBD crystal, one of which placed the DNA-binding surfaces of each monomer exactly one helical turn apart, and this was shown by mutational analysis to constitute the natural dimer (8). This contact was also present in several other crystal forms of BPV-1 E1-DBD. However, for the HPV-18 E1-DBD crystals, there was no apparent biologically relevant dimer from crystal packing. It should be noted that the same $\alpha 3$ helix interface was not used for lattice interactions, and therefore its different conformation is probably not due to crystal packing forces. The difference in the HPV-18 E1 $\alpha 3$ helix structure and the T-to-A transversion in the HPV-18 E1 binding site 2 (Table I) brought up the possibility that HPV-18 E1 dimerizes and/or contacts the DNA differently. To study E1/E1 and E1/DNA interactions, we performed the experiments described below.

The $\alpha 3$ Helix Is Important for Multimerization of the HPV-18 E1-DBD on DNA—Fluorescence anisotropy experiments per-

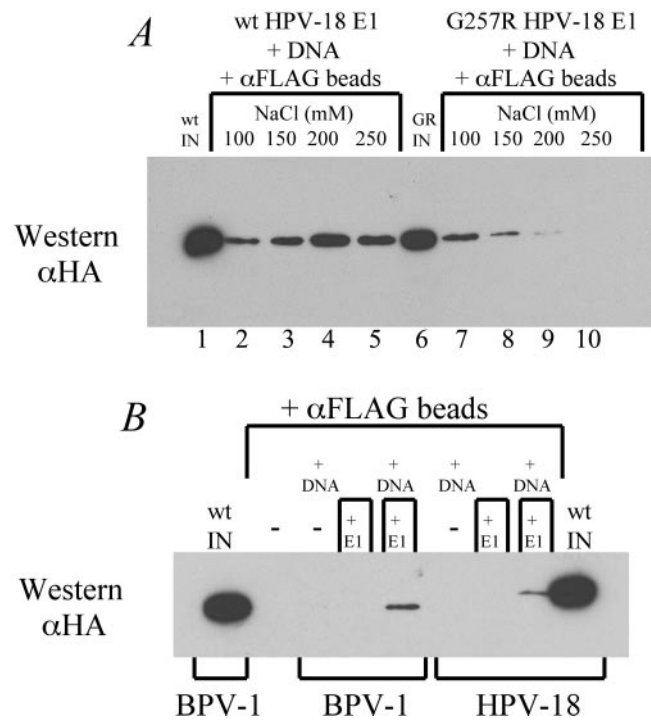


FIG. 3. **Mutations at the $\alpha 3$ helix affect DNA-dependent dimerization of HPV-18 E1-DBD in a salt-sensitive manner.** A, FLAG- and HA-tagged wild type (*wt*) (lanes 2–5) or $\alpha 3$ helix mutant HPV-18 E1-DBD (the G257R (*GR*) mutant is shown) (lanes 7–10) were mixed in the presence of DNA containing HPV-18 E1-BS and a range of salt concentrations (100–250 mM as indicated) and immunoprecipitated with an anti-FLAG antibody. Immunoprecipitates were analyzed by Western blot using an antibody specific for the HA tag. One-tenth of input (*IN*) is shown as a loading control (lanes 1 and 6). B, co-immunoprecipitation of FLAG- and HA-tagged wild type (*wt*) BPV-1 or HPV-18 E1-DBD in the presence of 100 mM salt, with and without DNA containing the respective E1-BS, to show the DNA dependence of dimerization. One-tenth of input (*IN*) is shown as a loading control.

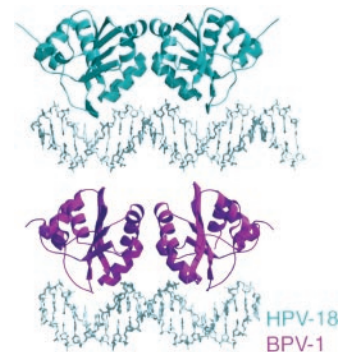


FIG. 4. **Comparison of the BPV-1 E1-DBD dimer with DNA crystal structure with an energy-minimized model of the HPV-18 E1-DBD dimer with DNA.** Two monomers of HPV-18 E1-DBD (cyan) were superimposed onto the BPV-1 E1-DBD dimer (magenta) structure docked onto an idealized B-form DNA containing HPV-18 E1-BS and energy-minimized with AMBER 7 (35).

formed with wild type BPV-1, HPV-11, and HPV-18 E1-DBD showed that E1-DBD preferentially binds DNA as a dimer in all cases (17). The surface involved in E1 dimerization was identified for BPV-1 as the $\alpha 3$ helix by mutagenesis (8) and

ribbon diagrams of the HPV-18 (left) and BPV-1 (right) E1-DBD crystal structures, color-ramped from red at the N terminus to magenta at the C terminus. The structures are shown side by side in the same view to appreciate the overall similarity of the fold. The disordered DNA-binding loop for HPV-18 E1-DBD is indicated by the dashed line. C, superposition of the HPV-18 (cyan) and BPV-1 E1-DBD (magenta) α -carbon traces, in the same view as B, to show the differences between the two structures. The regions that overlay with an r.m.s.d. of greater than 2 \AA are shown in color, and regions that align well (r.m.s.d. $< 2 \text{ \AA}$) are shown in gray. The disordered HPV-18 DNA-binding loop is indicated by the thin line.

A 21 bp Competitor DNA (unlabeled)

BPV-1	ATAA <u>TTGT</u> TGTT <u>ACA</u> AATAAT
wt	TATTA <u>ACA</u> CAA TTGT <u>TATTA</u>
HPV-18	ACA <u>ATTGT</u> TAAA <u>AGT</u> AATAAT
wt	TGTTAA <u>CA</u> ATTT TCAT <u>AATTA</u>
HPV-18	ACA <u>ATTGT</u> TAAA <u>AGT</u> AATAAT
A→T_{site2}	TGTTAA <u>CA</u> ATTT TCAT <u>TATTA</u>
HPV-18	ACA <u>AATGT</u> TAAA <u>AGT</u> AATAAT
T→A_{site4}	TGTTT <u>TACA</u> ATTT TCAT <u>AATTA</u>
Non specific	GTCTGACGGTCA GACTGACGG
	CAGACTGCCAGT CTGACTGCC

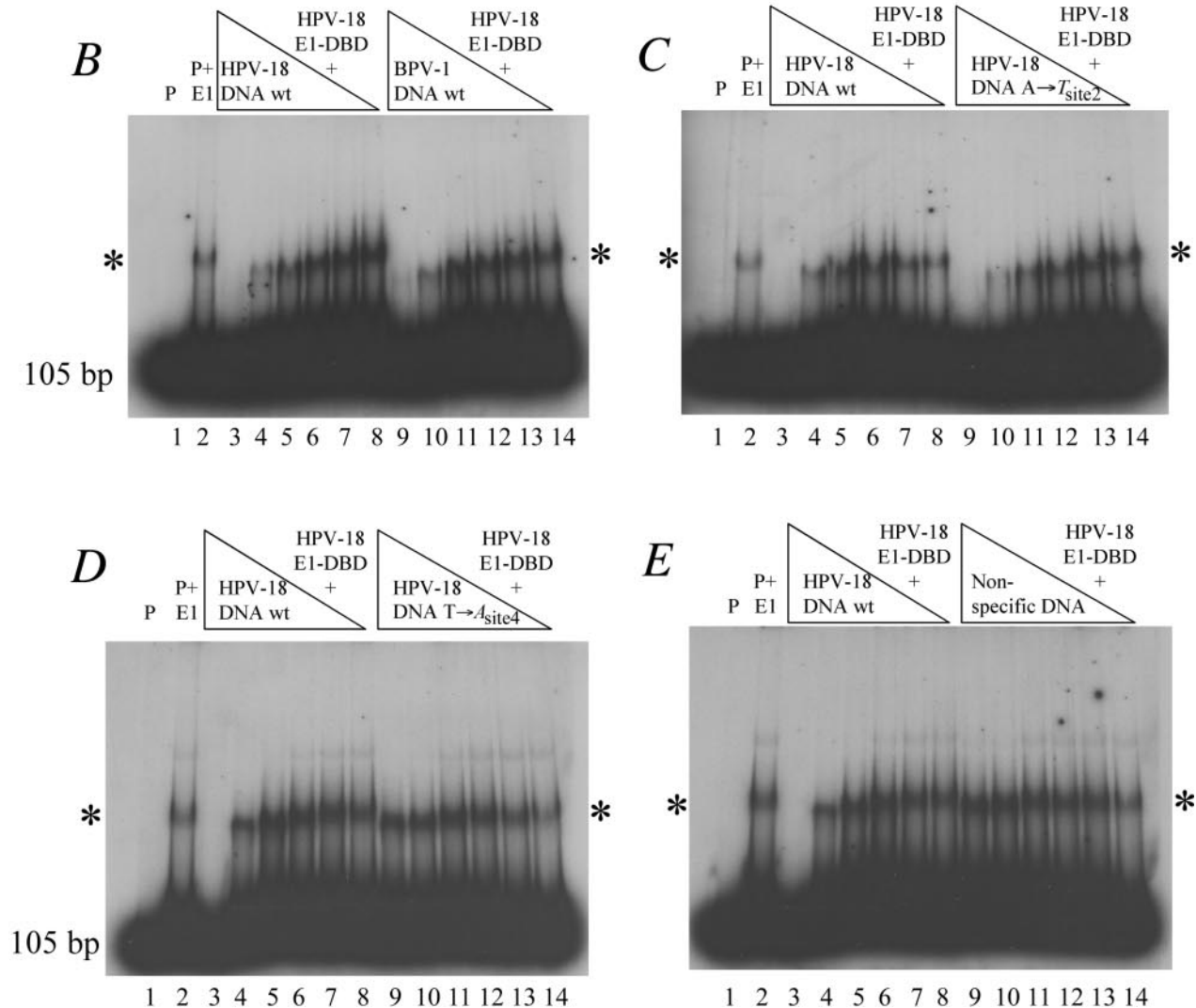


FIG. 5. **Demonstration of altered nucleotide specificity for HPV-18 E1-DBD by DNA competition.** A, sequences of unlabeled DNA used to compete complexes of 10 ng of wild type (*wt*) HPV-18 E1-DBD (*E1*) with 25,000 cpm/lane of a 105-bp HPV-18 *ori* probe (*P*). Nucleotides that form BS2 and -4, which encompass two consecutive major grooves of the DNA, are *underlined*. The nucleotide in position 2 of each BS is shown in *bold* typeface, and mutations are indicated by *italics*. For each competition assay, serial dilutions of the same stock DNA competitor concentration were used. The reactions were subjected to 5% PAGE and autoradiography. In all gels, *lane 1* is the radiolabeled *ori* probe alone, *lane 2* contains HPV-18 E1-DBD incubated with the *ori* probe, *lanes 3–8* contain 5-fold dilutions of unlabeled HPV-18 wild type (*wt*) E1-BS competitor incubated with HPV-18 E1-DBD and *ori* probe, and *lanes 9–14* contain 5-fold dilutions of unlabeled test competitor incubated with HPV-18 E1-DBD and *ori* probe.

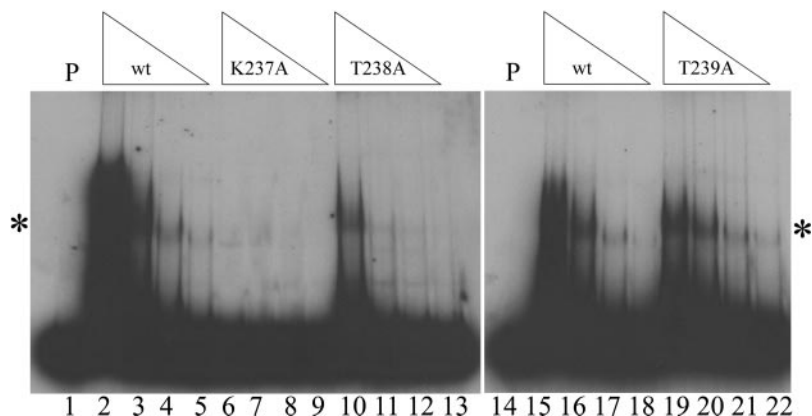


FIG. 6. Demonstration of altered residue requirements for HPV-18 E1-DBD by gel mobility shift analysis of DNA-binding loop mutants. DNA binding activities of wild type HPV-18 E1-DBD (*wt*) (lanes 2–5 and lanes 15–18) and the DNA-binding loop mutants (K237A, lanes 6–9; T238A, lanes 10–13; and T239A, lanes 19–22) were assayed with a 105-bp HPV-18 *ori* probe (*P*) that contains wild type E1-BS. Four 2-fold dilutions of the same stock concentration of each protein were used. The reactions were subjected to 5% PAGE and autoradiography. Probe alone is shown in lanes 1 and 14. The position of the band corresponding to the complex of HPV-18 E1-DBD and *ori* probe is indicated by the asterisks. In like manner to the analogous experiment performed with BPV-1 E1, the K237A mutation abolished E1 DNA binding activity, and the T239A mutation retained DNA binding activity as compared with wild type. However, in contrast to the analogous experiment with BPV-1 E1, the T238A mutation decreased E1 DNA binding activity as compared with wild type but did not abrogate it.

confirmed by the crystal structure of the BPV-1 E1-DBD dimer with DNA (15). Gel mobility shift assays with BPV-1 E1-DBD and fluorescence anisotropy experiments for HPV-11 E1-DBD revealed that substitution of a small hydrophobic residue in $\alpha 3$ helix to a bulky charged residue (e.g. A206R for BPV-1 or A251R for HPV-11) inhibits E1 from binding DNA as a dimer and instead promotes binding as a monomer (8, 17). The BPV-1 A206R² and HPV-11 A251R (17) full-length E1 mutants are also severely compromised for replication of *ori*-containing plasmids *in vivo*. While the functional importance of E1 dimerization has been demonstrated for BPV-1 and HPV-11, it has not been shown that the analogous residues required for BPV-1 and HPV-11 E1 dimerization are involved in HPV-18 E1 dimerization.

To assess whether HPV-18 E1-DBD binds DNA as a dimer via the same interface, the analogous substitutions in HA- and FLAG-tagged HPV-18 E1-DBD constructs were made by site-directed mutagenesis (G257R, I254R, and I254D). These mutations do not affect proper folding of these proteins since they were still able to bind DNA in a gel mobility shift assay, although higher mutant protein concentrations were required to obtain these complexes (data not shown).

E1 dimerization was assayed by mixing HA- and FLAG-tagged wild type or mutant proteins together with DNA, immunoprecipitating the proteins with anti-FLAG affinity gel, and subsequently performing Western blot analysis with anti-HA antibody. To overcome possible sequence-nonspecific protein/DNA interactions, which could lead to co-immunoprecipitation artifacts, the immunoprecipitation reactions were performed in the presence of a range of salt concentrations. The rationale was that higher salt concentrations would stabilize hydrophobic protein/protein interactions of cooperatively bound protein dimers at adjacent E1 binding sites, while destabilizing electrostatic protein/DNA interactions of independently bound monomers. As shown in Fig. 3A, co-immunoprecipitation of wild type HPV-18 E1 was stably maintained at

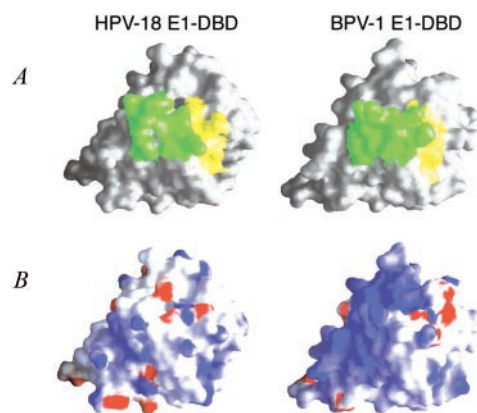


FIG. 7. Comparison of the electrostatic surface potential of the HPV-18 and BPV-1 E1-DBD DNA-binding surfaces. A, surface representation of HPV-18 (left) and BPV-1 (right) E1-DBD with the residues forming the DNA-binding loop mapped in green and the DNA-binding helix mapped in yellow. B, electrostatic potentials of the HPV-18 (left) and BPV-1 (right) E1-DBD molecular surfaces displayed in the same view as A as a color gradient from red (electronegative, $\le -10 k_B T$) to blue (electropositive, $\ge 10 k_B T$) where k_B is the Boltzmann constant and T is absolute temperature. These figures were drawn with the program GRASP (37) and are rotated by $\sim 90^\circ$ along the x axis with respect to the view in Fig. 1B to expose the DNA-binding surfaces.

increasing salt concentrations with an optimal NaCl concentration of 200 mM (lane 4). However, co-immunoprecipitation of the HPV-18 $\alpha 3$ helix mutant protein G257R was unstable under these assay conditions and did not occur at salt concentrations greater than 150–200 mM (compare lane 8 with 3, lane 9 with 4, and lane 10 with 5). Proteins did not co-immunoprecipitate in the absence of DNA (Fig. 3B). The experiment was highly reproducible ($n \geq 3$), and the same result was obtained with the other two $\alpha 3$ helix mutants, I254R and I254D (data not shown). These results indicate that $\alpha 3$ helix mutations do not affect the ability of independent monomers to bind DNA but

The position of the band corresponding to the complex of HPV-18 E1-DBD and *ori* probe is indicated by the asterisks. The effect of the identical concentration of wild type competitor is compared with that of each test competitor DNA (for each gel, compare lane 3 with 9, lane 4 with 10, lane 5 with 11, lane 6 with 12, lane 7 with 13, and lane 8 with 14). B, the relative affinity of HPV-18 E1-DBD for its own wild type (*wt*) E1-BS as compared with BPV-1 wild type E1-BS is similar. C, the relative affinity of HPV-18 E1-DBD for its own wild type E1-BS as compared with a mutant E1-BS in which the anomalous adenine in position 2 of BS2 is changed to thymidine (DNA A \rightarrow T_{site2}) is similar. D, HPV-18 E1-DBD has a higher affinity for its own wild type E1-BS than for a mutant E1-BS in which the thymidine in position 2 of BS4 is transverted to adenine (DNA T \rightarrow A_{site4}). E, HPV-18 E1-DBD has a higher affinity for its own wild type E1-BS than for nonspecific DNA.

do inhibit HPV-18 E1 dimerization and cooperative binding.

Since HPV-18 E1 dimerizes via an interface analogous to BPV-1 and HPV-11 E1 dimers, we constructed a model of the HPV-18 E1-DBD dimer by sequential superposition of two monomers of the protein on the structure of the BPV-1 E1-DBD dimer with DNA (LSQMAN (33)). In this model, each disordered DNA-binding loop was built in a conformation similar to that of BPV-1 E1. The HPV-18 E1-DBD dimer model was subsequently subjected to two rounds of energy minimization to relieve steric clashes (AMBER 7 (35)). This minimized HPV-18 model is shown in Fig. 4 in comparison with the crystal structure of the BPV-1 E1-DBD dimer complex with DNA (15) to demonstrate the obvious structural differences at the dimerization interface.

Affinity of the HPV-18 E1-DBD for Its Cognate Origin, BPV-1 E1 Binding Sites, or Mutant Sites—Sequence alignment of the respective origins of replication from HPV-18, other HPV types, and BPV-1 E1-BS revealed a potential difference in HPV-18 E1 DNA recognition (Table I). The only invariant base in the E1-BS (as shown for BPV-1 and HPV-11) is the conserved thymidine in position 2 of each BS (15, 17). However, as shown in Table I, the HPV-18 E1-BS has a T-to-A transversion at this position in BS2. We resequenced the HPV-18 *ori* several times and confirmed that the T-to-A transversion is indeed present in the HPV-18 E1-BS (data not shown).

When we superimposed the energy-minimized HPV-18 E1-DBD dimer model (Fig. 4) on the BPV-1 E1-DBD dimer structure, we observed a major difference in the alignment of the DNA-binding loops of each HPV-18 E1-DBD monomer (LSQMAN (33)) (data not shown). For the monomer in the HPV-18 E1-DBD dimer model that binds to E1-BS4 containing the invariant thymidine, the only α -carbons of the DNA-binding loop that do not superimpose well (r.m.s.d. > 2 Å) correspond to residues Lys-237 and Thr-238 (equivalent to BPV-1 Lys-186 and Thr-187). The α -carbons of the other residues of the DNA-binding loop in this monomer remained close to the conformation of the BPV-1 DNA-binding loop. In contrast, the monomer that binds to E1-BS2, which contains the T-to-A transversion, has a total of five adjacent α -carbons (residues 235–239) in the DNA-binding loop that do not align well with the equivalent BPV-1 E1-DBD α -carbons (residues 184–188). The α -carbons of these five residues are also positioned differently as compared with the DNA-binding loops in the HPV-18 input model used for energy minimization. The discrepancy between DNA-binding loops of HPV-18 E1-DBD monomers suggests that the HPV-18 E1-DBD dimer may bind to E1-BS2 and -BS4 in an asymmetric fashion.

To study HPV-18 E1-DBD DNA sequence specificity, we performed gel mobility shift assays in which E1-*ori* probe complexes were competed with unlabeled DNA. Sequences of competitor DNA are shown in Fig. 5A. E1 and DNA were incubated in the presence of 200 mM NaCl as we had determined in the immunoprecipitation experiments described above that this salt concentration optimizes specific E1/DNA interactions and minimizes sequence-nonspecific interactions. Similar relative affinities were obtained when competition was performed with HPV-18 wild type E1-BS compared with BPV-1 wild type E1-BS (Fig. 5B) or compared with mutant HPV-18 E1-BS in which the deviant adenine in position 2 was reverted back to the conserved thymidine (Fig. 5C) as the same concentration of each competitor DNA was required to achieve the same degree of competition (for both gels, compare lane 3 with 9 and lane 4 with 10). However, a mutant HPV-18 E1-BS in which an additional T-to-A transversion is introduced in position 2 of BS4 demonstrated a significantly diminished capacity to compete E1-*ori* complexes as compared with wild type HPV-18 E1-BS

(Fig. 5D, compare lane 9 with 3 and lane 10 with 4), suggesting that the thymidine in this site is important to DNA recognition. The binding of HPV-18 E1-DBD to the labeled probe was not competed with nonspecific DNA in the same concentration range as specific competitors (Fig. 5E, compare lane 9 with 3 and lane 10 with 4). These experiments indicate that in contrast to BPV-1 E1, which requires thymidine in position 2 of both BS2 and BS4 for DNA binding, sequence-specific HPV-18 DNA recognition is dependent only on the thymidine in BS4.

Residue Requirements in the HPV-18 E1 DNA-binding Loop—The crystal structure of the BPV-1 E1-DBD dimer in complex with DNA revealed that, as in most DNA-binding proteins, E1/DNA interactions are mostly electrostatic. However, unlike most DNA-binding proteins, all base-specific contacts in this case are van der Waals interactions. These base-specific contacts all involve residues of the DNA-binding loop, and most are to the thymidine in position 2 of each hexanucleotide site (15). The role of the BPV-1 DNA-binding helix in nonspecific DNA contacts is supported by the tolerance for mutational changes in this α -helix (36). However, mutational analysis of the BPV-1 E1 DNA-binding loop revealed that in addition to several charged residues (Arg-180, Lys-183, and Lys-186), one threonine in the loop (Thr-187) is also critical for DNA binding, while the neighboring threonine (Thr-188) is not (22). Thr-187 was shown in the crystal structure of the BPV-1 E1-DBD dimer and tetramer with DNA to be one of the major contacts of the invariant thymidine in position 2 of the E1-BS (15).

To see whether there is a difference in residue requirements for HPV-18 E1 DNA binding, we cloned and purified the equivalent DNA-binding loop mutant proteins (HPV-18 K237A, T238A, and T239A equivalent to BPV-1 Lys-186, Thr-187, and Thr-188) and performed the analogous gel mobility shift assay. Serial 2-fold dilutions of the same stock protein concentrations were tested for *ori* binding activity. As evident in Fig. 6, a mutation of Lys-237 to alanine completely abrogated HPV-18 E1 DNA binding activity (compare lanes 6–9 with lanes 2–5). This parallels the result that was obtained with the equivalent BPV-1 K186A mutant. Similarly the HPV-18 T239A mutant retained wild type DNA binding activity (compare lanes 19–22 with lanes 2–5), which also parallels the result obtained for the equivalent BPV-1 mutant (T188A). However, while the BPV-1 T187A mutation completely abolished DNA binding activity, the equivalent HPV-18 T238A mutation showed only a reduction in *ori* binding (compare lanes 10–13 with lanes 2–5). This result may be related to the loss of the thymidine requirement in position 2 of the HPV-18 E1-BS.

DISCUSSION

In the present study we describe structural and biochemical studies of E1-DBD from a clinically relevant, high risk human papillomavirus (HPV-18) that may facilitate the development of targeted antiviral agents at benign and premalignant stages of disease. The E1 dimerization interface is a logical target for the disruption of DNA replication by a small molecule because of its limited surface area and importance for binding of E1 to DNA and for viral DNA replication. However, to date there are no reported structures of the E1-DBD from any HPV.

Here we describe the structure refined to 1.8-Å resolution of the E1-DBD from HPV-18 and show that one major structural difference in comparison with the BPV-1 E1-DBD lies in the α 3 helix, which forms the E1 dimerization interface. In the HPV-18 E1-DBD, the α 3 helix is kinked due to ($n + 3$) backbone H-bonding interactions and a tightly bound solvent molecule, resulting in a partial 3_{10} helix, while the BPV-1 E1-DBD α 3 helix retains the ($n + 4$) H-bonding network of a typical helix with no bound solvent. Because of this difference in one of the

key functional elements of the protein, immunoprecipitation experiments were performed to demonstrate that the analogous residues required for BPV-1 and HPV-11 E1 dimerization are also required for HPV-18 E1 dimerization. This structural difference is relevant to drug design at the E1 dimerization interface and may also play a role in stability of HPV-18 E1-DNA complexes by forming tighter dimers and/or positioning the DNA binding elements differently as compared with BPV-1 E1.

Importantly the HPV-18 E1-BS has a T-to-A transversion in an otherwise invariant nucleotide position (Table I). In addition, the DNA-binding loop of HPV-18 E1-DBD was disordered in the crystal structure. Therefore, we performed gel mobility shift assays to study the nucleotide sequence and residue requirements for HPV-18 E1 DNA binding. We found that HPV-18 E1-DBD does not share the same requirements for DNA recognition as BPV-1 and HPV-11 E1 (Figs. 5 and 6). The thymidine in position 2 of BS2 and the threonine that was shown for BPV-1 to be the major contact of this nucleotide are both nonessential for HPV-18, although the thymidine in position 2 of BS4 does play a role in HPV-18 E1 DNA recognition.

However, discrimination of E1-BS does not just rely on direct base contacts. Other key determinants of E1-BS recognition include electrostatic interactions and structural features of DNA such as backbone flexibility. The BPV-1 E1-DBD was shown to distort the DNA in co-crystal structures and biochemical studies (15, 20), and this E1-induced DNA deformation involves additional stretches of sequence outside the E1-BS (21). While these flanking regions demonstrated tolerance for mutations, suggesting that these contacts are phosphate backbone interactions and not base-specific, the contacts are nonetheless critical for stabilizing the E1-DNA complex and bending the DNA around the protein (21). The contacts within the E1-BS were also shown to be primarily nonspecific phosphate backbone interactions with mutational tolerance (15, 36). Because of the predominance of electrostatic interactions in BPV-1 E1 DNA binding, we mapped the electrostatic potential of the DNA-binding surfaces of the BPV-1 and HPV-18 E1-DBD for comparison. For HPV-18 E1-DBD, the disordered DNA-binding loop was modeled in a conformation similar to that of BPV-1 E1. As shown in Fig. 7, the shapes and locations of the charged patches of surface potential are different for BPV-1 and HPV-18, suggesting specific energetic coupling between each protein, its respective BS, and the flanking DNA.

There is evidence from BPV-1 that E1 also has a sequence-dependent structural requirement in the DNA. The BPV-1 E1-BS was observed to contain a 2-fold symmetrical pattern of the most kinkable pyrimidine-purine steps (TG, CA, and TA) at three base intervals (15). The increased positive rise, twist, and slide of the DNA and the highly negative roll observed in the BPV-1 E1-DBD-DNA complex structures were most pronounced at the central dinucleotide step (15). However, this same pattern of pyrimidine-purine steps is not completely conserved among all the other papillomavirus E1-BS sequences as every HPV sequence lacks at least one kinkable dinucleotide step (see Table I). The role of flexible dinucleotide steps in other E1-BSs, as studied by mutational tolerance in HPV-11, is unclear (17). It is interesting to note that for the HPV-18 E1-BS, the symmetrical, regularly spaced pattern of pyrimidine-purine steps as found in BPV-1 is maintained except for the central dinucleotide step, which is a rigid purine-purine. The rigid central dinucleotide step and the T-to-A transversion in E1-BS2 may both alter the kinkability and conformation of the HPV-18 E1-BS. There may be different requirements for local DNA flexibility for HPVs as compared with BPV-1 because, while in HPV origins of replication the E1- and E2-BS are

distal (over 30 bp apart), in BPV-1 the E1- and E2-BS are proximal (only 3 bp apart). As a result, there is a required additional interaction in BPV-1 between the DBDs of E1 and E2 that does not occur in HPV (38). This interaction induces a sharp bend in the BPV-1 *ori* (120–130°) and facilitates the productive interaction between the BPV-1 E1 helicase domain and E2 activation domain (20).

It was presented here that the DNA-binding loop in the HPV-18 E1-DBD structure is disordered when unbound, so the conformation of the loop is unknown. It is possible that the residues of the HPV-18 E1 DNA-binding loop could shift position to accommodate variations in geometric parameters of the DNA as compared with BPV-1 E1. Our energy-minimized model of the HPV-18 E1-DBD dimer in complex with DNA (Fig. 4) suggests that HPV-18 E1 DNA recognition may be asymmetric as the conformation of the DNA-binding loop of each monomer is not entirely superimposable.

Taken together, several features of HPV-18 E1-DBD may contribute to the complementarity between the protein and its E1-BS: the kinked $\alpha 3$ helix, the conformation(s) for the DNA-binding loops of each monomer in the dimer, and the electrostatic potential of the DNA-binding surface. As variations in the sequence-specific kinkability of the E1-BS DNA and flanking sequences can also contribute to complementarity, E1 *ori* recognition likely involves an indirect readout mechanism as well. Indirect readout, a reliance on structural features of DNA, has been hypothesized as a mechanism of DNA recognition for a number of other DNA-binding proteins (39), including the papillomavirus E2 protein (40). A more detailed understanding of the interaction between HPV-18 and its binding site await further structural studies of a complex between the two.

Acknowledgments—We thank Dr. Arne Stenlund for providing the HPV-18 E1-DBD (residues 210–354) expression plasmid, for critical reading of the manuscript, and for helpful discussions; Seth Bechis for initial screening of crystallization conditions; Dr. Annie Heroux at beamline X26C and Dr. Paul O'Farrell for assistance with data collection at the National Synchrotron Light Source at Brookhaven National Laboratory; Ashish Saxena for reagents; Drs. Carlos Simmerling and Rajesh Kumar for help and advice with AMBER 7; and Dr. Eric Enemark for critical reading of the manuscript.

REFERENCES

- Walboomers, J. M., Jacobs, M. V., Manos, M. M., Bosch, F. X., Kummer, J. A., Shah, K. V., Snijders, P. J., Peto, J., Meijer, C. J., and Munoz, N. (1999) *J. Pathol.* **189**, 12–19
- Bosch, F. X., and de Sanjosé, S. (2003) *J. Natl. Cancer Inst. Monogr.* **31**, 3–13
- Crum, C. P., Abbott, D. W., and Quade, B. J. (2003) *J. Clin. Oncol.* **21**, 224–230
- Cullen, A. P., Reid, R., Campion, M., and Lorincz, A. T. (1991) *J. Virol.* **65**, 606–612
- Sanders, C. M., and Stenlund, A. (1998) *EMBO J.* **17**, 7044–7055
- Lusky, M., Hurwitz, J., and Seo, Y.-S. (1994) *Proc. Natl. Acad. Sci. U. S. A.* **91**, 8895–8899
- Wilson, V. G., West, M., Woytek, K., and Rangasamy, D. (2002) *Virus Genes* **24**, 275–290
- Enemark, E. J., Chen, G., Vaughn, D. E., Stenlund, A., and Joshua-Tor, L. (2000) *Mol. Cell* **6**, 149–158
- Campos-Olivas, R., Louis, J. M., Clérot, D., Gronenborn, B., and Gronenborn, A. M. (2002) *Proc. Natl. Acad. Sci. U. S. A.* **99**, 10310–10315
- Hickman, A. B., Ronning, D. R., Kotin, R. M., and Dyda, F. (2002) *Mol. Cell* **10**, 327–337
- Chen, G., and Stenlund, A. (1998) *J. Virol.* **72**, 2567–2576
- Stenlund, A. (2003) *EMBO J.* **22**, 954–963
- White, P. W., Titolo, S., Brault, K., Thauvette, L., Pelletier, A., Welchner, E., Bourgon, L., Doyon, L., Ogilvie, W. W., Yoakim, C., Cordingley, M. G., and Archambault, J. (2003) *J. Biol. Chem.* **278**, 26765–26772
- Sanders, C. M., and Stenlund, A. (2000) *J. Biol. Chem.* **275**, 3522–3534
- Enemark, E. J., Stenlund, A., and Joshua-Tor, L. (2002) *EMBO J.* **21**, 1487–1496
- Fouts, E. T., Yu, X., Egelman, E. H., and Botchan, M. R. (1999) *J. Biol. Chem.* **274**, 4447–4458
- Titolo, S., Brault, K., Majewski, J., White, P. W., and Archambault, J. (2003) *J. Virol.* **77**, 5178–5191
- Sedman, T., Sedman, J., and Stenlund, A. (1997) *J. Virol.* **71**, 2887–2896
- Chen, G., and Stenlund, A. (2001) *J. Virol.* **75**, 292–302
- Gillitzer, E., Chen, G., and Stenlund, A. (2000) *EMBO J.* **19**, 3069–3079
- Chen, G., and Stenlund, A. (2002) *Mol. Cell. Biol.* **22**, 7712–7720
- Gonzalez, A., Bazaldua-Hernandez, C., West, M., Woytek, K., and Wilson, V. G. (2000) *J. Virol.* **74**, 245–253

23. Otwinowski, Z., and Minor, W. (1997) *Methods Enzymol.* **276**, 307–326
24. Vagin, A., and Teplyakov, A. (2000) *Acta Crystallogr. Sect. D Biol. Crystallogr.* **56**, 1622–1624
25. Brünger, A. T., Adams, P. D., Clore, G. M., DeLano, W. L., Gros, P., Grosse-Kunstleve, R. W., Jiang, J.-S., Kuszewski, J., Nilges, M., Pannu, N. S., Read, R. J., Rice, L. M., Simonson, T., and Warren, G. L. (1998) *Acta Crystallogr. Sect. D Biol. Crystallogr.* **54**, 905–921
26. Jones, T. A., Zou, J. Y., Cowen, S. W., and Kjeldgaard, M. (1991) *Acta Crystallogr. Sect. A* **47**, 110–119
27. Kleywegt, G. J., Zou, J. Y., Kjeldgaard, M., and Jones, T. A. (2001) in *International Tables for Crystallography, Vol. F. Crystallography of Biological Macromolecules* (Rossman, M. G., and Arnold, E., eds) pp. 353–356, 366–367, Kluwer Academic Publishers, Dordrecht, The Netherlands
28. Kraulis, P. J. (1991) *J. Appl. Crystallogr.* **24**, 946–950
29. Esnouf, R. M. (1997) *J. Mol. Graph.* **15**, 132–134
30. Bacon, D. J., and Anderson, W. F. (1988) *J. Mol. Graph.* **6**, 219–220
31. Merritt, E. A., and Murphy, M. E. P. (1994) *Acta Crystallogr. Sect. D Biol. Crystallogr.* **50**, 869–873
32. Carey, M., and Smale, S. T. (2000) *Transcriptional Regulation in Eukaryotes. Concepts, Strategies, and Techniques*, Cold Spring Harbor Laboratory, pp. 257–268, Cold Spring Harbor, NY
33. Kleywegt, G. J., and Jones, T. A. (1997) *Methods Enzymol.* **277**, 525–545
34. McDonald, I. K., and Thornton, J. M. (1994) *J. Mol. Biol.* **238**, 777–793
35. Case, D. A., Pearlman, D. A., Caldwell, J. W., Cheatham, T. E., Wang, J., Ross, W. S., Simmerling, C., Darden, T., Merz, K. M., Stanton, R. V., Cheng, A., Vincent, J. J., Crowley, M., Tsui, V., Gohlke, H., Radmer, R., Duan, Y., Pitera, J., Massova, I., Seibel, G., Singh, U. C., Weiner, P., and Kollman, P. A. (2002) *AMBER 7*, University of California, San Francisco
36. West, M., Flanery, D., Woytek, K., Rangasamy, D., and Wilson, V. G. (2001) *J. Virol.* **75**, 11948–11960
37. Nicholls, A., Sharp, K. A., and Honig, B. (1991) *Proteins* **11**, 281–296
38. Berg, M., and Stenlund, A. (1997) *J. Virol.* **71**, 3853–3863
39. Dickerson, R. E. (1998) *Nucleic Acids Res.* **26**, 1906–1926
40. Zimmerman, J. M., and Maher, L. J., III (2003) *Nucleic Acids Res.* **31**, 5134–5139